Nuclear Instruments and Methods in Physics Research A256 (1987) 323–328
North-Holland, Amsterdam

CRYSTAL REFLECTIVITY FOR BENT CRYSTAL SPECTROMETERS

E. KAERTS * and P.H.M. VAN ASSCHE *

IKS, Leuven University, 3030 Leuven, Belgium and SCK/CEN, 2400 Mol, Belgium

G.L. GREENE and R.D. DESLATTES

National Bureau of Standards, Gaithersburg, MD 20899, USA

Received 7 January 1987

The reflectivity properties of a bent silicon crystal, used as the diffraction crystal in a transmission type Bent-Crystal Diffraction (BCD) spectrometer, were investigated. In particular the energy dependence of the integrated reflecting power was studied. It was found that the integrated reflecting power stayed constant up to unexpectedly high energies, depending on the diffraction order and on the quality of the crystal bending. Beyond an inflexion point this reflecting power decreased with only E^{-1} instead of E^{-2} with quartz crystals. Both this diffraction behaviour and the improved energy resolution extend the usefulness of bent-crystal diffraction spectrometers beyond 1 MeV gamma ray energy. The results are discussed and interpreted in terms of the diffraction theory for perfect crystals.

1. Introduction

Both the utility and the limitations of a Bent-Crystal Diffraction (BCD) spectrometer depend principally on the behaviour of the analysing crystal. The requirement for high precision implies simultaneously a high reflecting power and a very small diffraction line width. The availability of strong higher order reflections permit multiple order spectroscopy. A study of large crystals for BCD spectrometers, by Jacobs [1], Jacobs and Hart [2] showed that the use of highly perfect silicon crystals instead of the traditionally used quartz crystals could substantially improve both spectrometer efficiency and energy resolution. Through its reflectivity behaviour, the crystal determines the high energy limit of the spectrometer.

A useful parameter for describing this reflectivity behaviour is the integrated reflecting power R. It is proportional to the area under the diffraction profile, namely:

$$R = \int \frac{I(\theta)}{I_0}\, \mathrm{d}\theta,$$

where I_0 is the intensity in the direct beam after passage through the crystal and the integration is taken over the diffraction profile. R is an intrinsic crystal property and depends on photon energy. A clear example is given by the two bent quartz crystals as used in the GAMS spectrometers at the ILL high flux reactor in Grenoble [3]. For γ-energies below 150 keV (350 keV) in the 4 mm (13 mm) case, the integrated reflecting power is a constant. For γ-energies above these values, the integrated reflecting power shows an E^{-2} energy dependence resulting in a corresponding decrease of the sensitivity of the instruments. These results differ from those expected for a perfect crystal. Such a specimen is being used in the BCD spectrometer installed at the SCK/CEN BR2 reactor in Mol, Belgium. We report results from this installation in the present communication.

2. Experimental

The crystal, a dislocation free slab of silicon, with dimensions $82 \times 60 \times 3.5$ mm^3, was clamped between two cylindrically ground blocks of 10.650 m radius with a window of 42 mm diameter. No supplementary films were placed between the crystal and the blocks. Two sets of blocks plus crystal were tested. In the first set, the crystal was clamped between two steel blocks which had an overall precision of 0.5 μm. In the second set, a stabilised copper alloy was used as material for the blocks. The deviations from the ideal curvature in the latter case were in the order of 0.1 μm. The two crystals were cut from the same cylindrical (82 mm diameter) ingot and were mechanically polished to an optical flatness better than 0.2 μm [2].

The quality of the bending could be controlled by

* Mailing Adress: S.C.K./C.E.N, BR1, Boeretang 200, B-2400 Mol, Belgium.

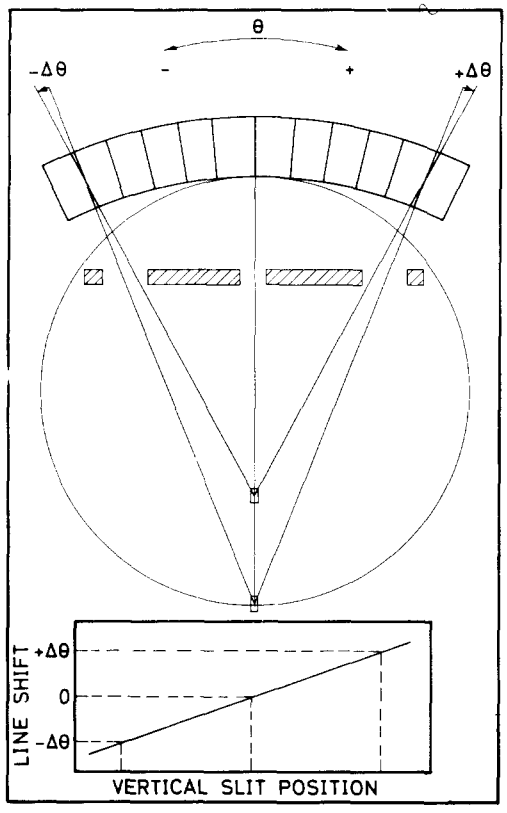

Fig. 1. Geometry of the transmission curved crystal spectrometer (DuMond geometry) illustrating the linear shift which arises when the source does not lie on the Rowland circle.

scanning the crystal aperture with a narrow (5 mm) slit. If the crystal was bent with a uniform radius of curvature, and a line shaped source was placed on the focal (Rowland) circle parallel to the diffracting crystal planes, the Bragg condition would be fulfilled at the same time at all places of the crystal for only one energy. In this ideal configuration, the peak position of the experimental diffraction line does not depend on which part of the crystal is selected by a narrow vertical aperture. When the source is not on the focal circle, an experimental line shift is observed when different parts of the crystal are selected by the vertical slit. The situation for too small a radius of curvature is shown in fig. 1. As can be seen, the expected shifts are linear. If however, the curvature is not uniform, a non linear shift is expected. For optimal bending, both the diffracting crystal planes and the symmetry axis of the clamping blocks are parallel. Experimentally, it is seen that misorientation of the crystal between the blocks entails a shift of the peak position when different narrow horizontal parts of the crystal are selected for diffraction. Ultimately, only that part of the crystal for which both a horizontal and a vertical scan results in a constant peak position of the diffraction line, is used. If a line source is employed, the shape of the diffraction line will be symmetrical.

For the first set of bending blocks (steel), the energy dependence of the first order integrated reflecting power R was measured using γ-transitions following the ground state decay of both ^{152}Eu ($T_{1/2} = 13.3$ yr) and ^{154}Eu ($T_{1/2} = 8.8$ yr). Only those transitions that could be measured in both the diffracted and the direct beam were considered. With this restriction we avoided corrections for absorption and detector efficiency. A total of ten measuring points between 100 and 1450 keV were selected. The intensities of the second order diffraction, relative to the first order, were obtained from measurement on natural europium. To determine for the second set the relative intensities for the higher order diffractions, the diffraction lines of 18 strong prompt γ-transitions from the reaction ^{164}Dy(n, γ)^{165}Dy were measured in the first four diffraction orders. The energies of these γ-transitions lay between 50 and 1100 keV.

5. Results

As explained earlier, the quality of the crystal bending can be determined experimentally. For the first set of clamping blocks, this was only done after the measurements for the integrated reflecting power were performed and only a vertical scanning has been used. It was found that the crystal was not uniformly bent and that for a displacement of the slit (opening 5 mm) of 2.5 cm, the peak position of the diffraction line shifted over an angle of 10″. The fwhm varied between 2.4″ and 2.8″.

The quality of the bending between the second set of clamping blocks was optimised before the measurements were done. Because of mechanical relaxations, this bending was repeated several times.

Some of the results of this optimisation are shown in figs. 2 and 3. In fig. 2, experimental line shifts as a function of the vertical aperture position are plotted for different source-to-crystal distances. It appears that only the central part of the crystal (opening between 0.5 and 2.5 cm) has a uniform curvature. This same situation ocurred every time the crystal was rebent. Consequently, only the central part of the crystal was selected for diffraction in the BCD spectrometer. The optimal source-to-crystal distance for this bending was found to be 1070 cm. Fig. 3 shows the experimental line shifts as a function of the horizontal aperture position for two different crystal orientations between the clamping blocks. The crystal orientation is defined relative to the upper side of the clamping blocks. As can be seen, its influence on the line shift is considerable.

In the case of the steel clamping blocks, a relative value for the first order integrated reflecting power R at

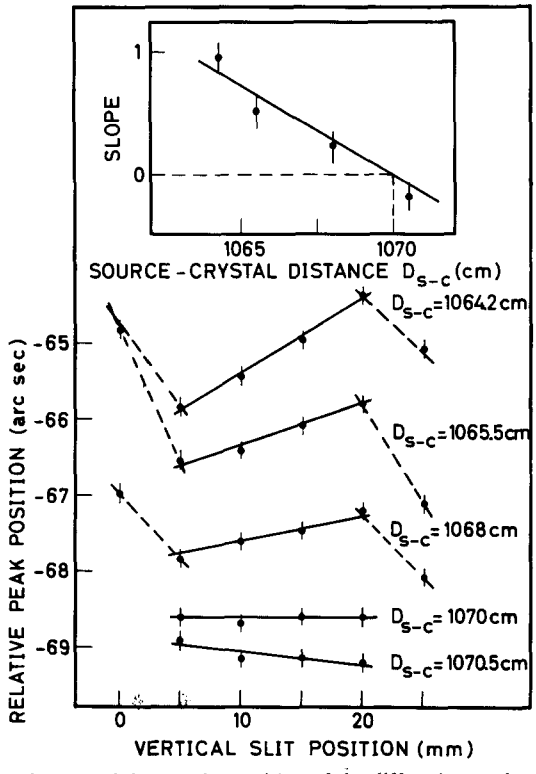

Fig. 2. Scan of the angular position of the diffraction peak as a function of vertical slit displacement. A linear dependence corresponds to a uniform crystal bend. Zero slope corresponds to the source lying on the Rowland circle.

a certain energy can be expressed as:

$$R = \frac{1}{I_0} \sum_j I_j ,$$

where I_0 is the intensity in the direct beam after passage through the crystal and the summation goes over the diffraction profile. Together with the ratio of the second to first order diffracted intensities, the relative integrated reflecting powers of the first two diffraction orders can be obtained for the first set of bending blocks. This result is shown in fig. 4. Because we are primarily interested in the energy dependence of the reflectivity, no attempt was made to obtain absolute values. The data points are normalised to 1.0 for the flat region of the first order reflectivity. The energy dependence of the first order integrated reflecting power between 400 and 1408 keV was found to be E^{-1} while for the second order an $E^{-1.5}$ dependence was found. The energies (in a log, log plot) for which the slope of R changes, are called "inflexion" points. The inflexion points in the first and second order curves appear around 400 and 220 keV respectively.

Assuming that the observed energy dependence is characteristic of bent Si(220) crystals in general, information about the locations of inflexion points in different diffraction orders can also be obtained by measuring the ratio of the higher to the first order diffracted intensities as functions of the photon energy. Fig. 5 shows results for both sets of clamping blocks.

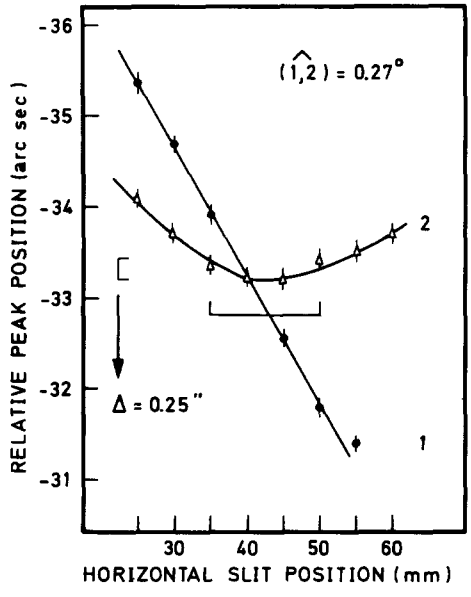

Fig. 3. Angular position of diffraction peak versus horizontal slit displacement.

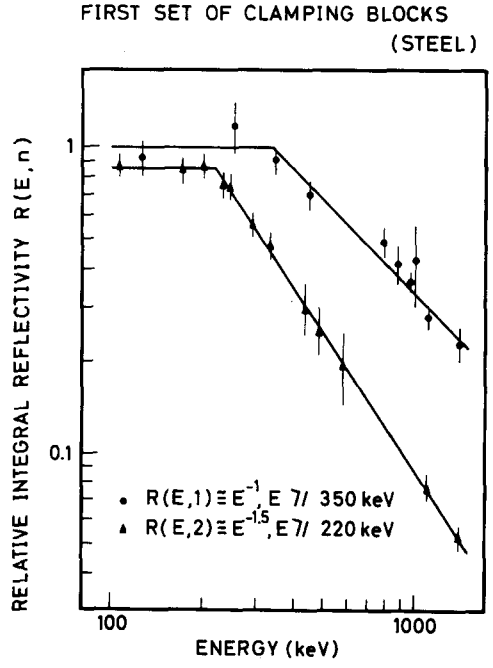

Fig. 4. Normalized integrated reflecting power versus energy for the steel clamping blocks.

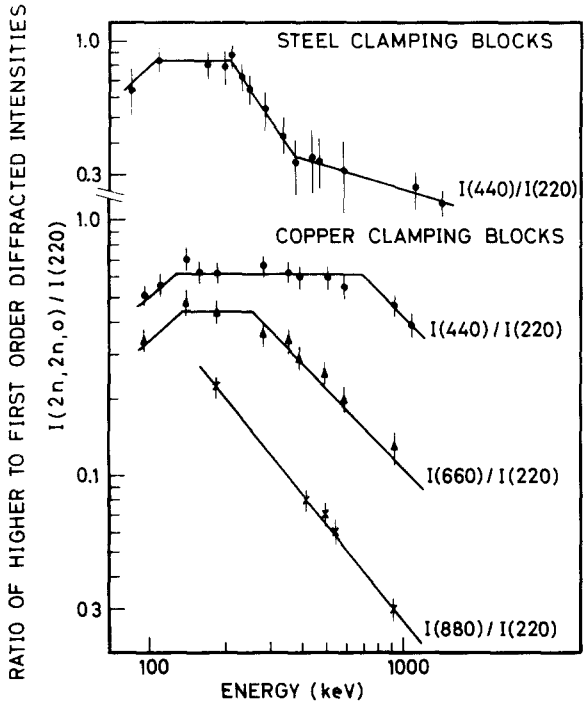

Fig. 5. Integrated reflecting powers for higher orders (normalized to [220]) as a function of energy for both sets of clamping blocks.

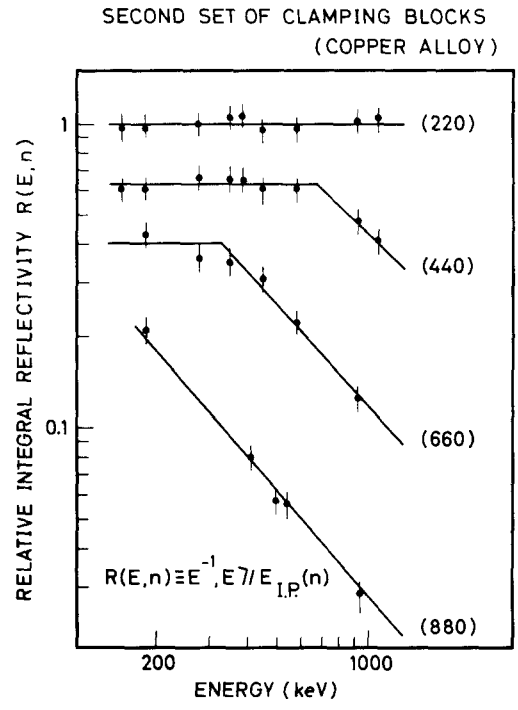

Fig. 6. Integrated reflecting power for several orders normalized to [220] for the copper alloy clamping blocks.

For the second set of clamping blocks, only one inflexion point is seen in the second and the third order curves while for the fourth order, no inflexion point is seen at all (in the energy range displayed). This seems to indicate that the first order integrated reflecting power of the bent Si(220) crystal with the second set of clamping blocks is a constant up to an energy of at least 1100 keV. We can now construct the integrated reflecting power for the first four diffraction orders from these measurements.

Relative values for R can be obtained from the following relation:

$$\frac{R(E, n)}{R(E_0, n_0)} = \frac{I(E, n)(1 - S(E_0))T(E_0)\epsilon(E_0)I_\gamma(E_0)}{I(E_0, n_0)(1 - S(E))T(E)\epsilon(E)I_\gamma(E)},$$

where n is the diffraction order, $I(E, n)/I(E_0, n_0)$ is the observed ratio of counts in the detector, $T(E)$ and $S(E)$ are respectively the transmission through the crystal and the self-absorption in the source derived from the atomic absorption coefficients, $I_\gamma(E)$ is the relative intensity of the γ-line and $\epsilon(E)$ is the efficiency of the NaI detector. For energies above 150 keV the absorption effects may be neglected. Ratios were determined with n_0 equal to one and with E_0 equal to 279.8 keV. The results are plotted in fig. 6. The first order integrated reflecting power vs energy curve shows indeed no inflexion point below 1100 keV. The energy dependences of the integrated reflecting powers in fourth order and above the inflexion points in second ($E = 680$ keV) and in third ($E = 300$ keV) order shows E^{-1} behaviour.

In the course of this analysis, the fwhm of the diffraction peaks were estimated. Table 1 shows the results for a few energies. It should be noted that the dominant contribution to this line width arises from the finite angular extent of the source. A typical source has

Table 1
Fwhm (arc sec) for energies between 50 and 1100 keV measured in different diffraction orders

Energy (keV)	order 1	order 2	order 3	order 4
50.4	3.1	3.1	–	–
94.7	1.9	1.6	1.7	–
108.2	1.9	1.6	–	–
139.1	1.5	1.6	1.3	–
184.3	1.4	1.2	1.4	1.3
361.7	1.4	1.4	1.4	1.3
496.9	1.3	1.2	1.2	1.3
912.0	1.2	1.2	1.0	1.1
1072.2	1.1	1.1	–	–

a width of ≈ 50 μm which at a distance of ≈ 10 m implies a diffraction width of 1895×10^{-6} rad (1″). As we shall discuss in the following section, the intrinsic width of the crystal is much less than this.

4. Discussion

While the theory for the diffraction of radiation by flat perfect crystals is well understood, [4] the theory of diffraction in deformed perfect crystals is less clear. In particular, any attempt to explain the behaviour of a particular real bent crystal is hampered by the great difficulty in describing the precise microscopic deformation of the crystal lattice. This deformation is complicated, anisotropic and depends on the details of the method by which the crystal is deformed. In particular, the behaviour of the crystal cannot be described simply in terms of the local radius of curvature in the plane of dispersion. Sumbayev [5] has shown that a bent, initially perfect, crystal will behave as a "quasimosaic" crystal with a mosaic "width", $\Delta\theta_{\text{mosaic}}$ given by:

$$\Delta\theta_{\text{mosaic}} \approx 2Kt,$$

where t is the thickness of the crystal and K is a local deformation parameter which may be viewed as $1/2r$ where r is the local radius of curvature of the *lattice planes*. Such a radius of curvature may arise, for example, for a nonideal bend or anisotropic terms in the elasticity tensor. In any real bent crystal it will be difficult to deduce K from a knowledge of only the mean macroscopic radius of curvature in the plane of dispersion.

Following the analysis of Sumbayev we may refer to this effect as "quasimosaic" to distinguish it from the more familiar mosaicity arising from random mis-orientation of perfect crystallites in a large nonperfect sample. In the more familiar mosaic case, perfect crystal "blocks" are assumed to be randomly distributed around some mean orientation. The "quasimosaic" crystal behaves as though the thin lamina comprising the crystal are rotated uniformly with depth at a rate such that the total angular displacement between the crystal planes at the front and rear surfaces of the crystal is equal to $\Delta\theta_{\text{mosaic}}$. This distinction is important since it implies a uniform "filling" of the diffraction width in the case of the quasimosaic as opposed to the statistical (assumed Gaussian) spread in familiar mosaic case.

This "quasimosaic" width may be compared with the "dynamical" width which results from the diffraction of radiation from a thick perfect flat crystal [4]. This width which we call $\Delta\theta_{\text{dynamic}}$ is given by

$$\Delta\theta_{\text{dynamic}} = \frac{\pi}{2}\frac{d}{t_e},$$

where d is the grating spacing and t_e is the primary extinction length. In the limit $\lambda \ll d$ this extinction length may be expressed by

$$t_e = \frac{V_0}{r_e \lambda F_H},$$

where V_0 is the unit cell volume, r_e, the classical radius of the electron and F_H is the crystal structure factor including the Debye–Waller term. Because of its dependence on λ^{-1}, the extinction length at any energy can be expressed as $t_e = t_1 E$ where numerically t_1 is the extinction length at 1 MeV and E is the energy of the radiation expressed in MeV. Table 2 gives the relevant parameters for the reflections on which we are reporting.

For a specified energy and reflection it is convenient to consider the ratio of the quasi-mosaic width to dynamical width. This, of course, is the number of ideal thick crystal widths required to "fill" the mosaic. If the crystal is sufficiently thick that $t/t_e \gg (\Delta\theta_{\text{mosaic}}/\Delta\theta_{\text{dynamic}})$ the entire crystal will appear thick in the sense that all radiation within the rocking curve ($\Delta\theta_{\text{mosaic}}$) will encounter many extinction lengths of crystal sufficiently close to the Bragg condition to insure reflection. Thus one expects a constant reflectivity as a function of E. However if $t/t_e \ll (\theta\,\Delta_{\text{mosaic}}/\Delta\theta_{\text{dynamic}})$, the overall crystal will appear "thin" in the sense that the radiation does not encounter a full extinction lenght. In this case we expect the integrated reflectivity to fall as E^{-1} (ref. [4]). Clearly the transition from constant reflectivity to E^{-1} reflectivity occurs in the vicinity of $t/t_e \approx \Delta\theta_{\text{mosaic}}/\Delta\theta_{\text{dynamic}}$, where t is the actual crystal thickness given by $t = 3.5$ mm.

By observing the energy at which this "inflexion point" occurs it is possible to estimate the quasimosaic width. Using a critical energy of 680 keV for the Si [440] reflection we infer $\Delta\theta_{\text{mosaic}} \approx 1.1 \times 10^{-6}$. This agrees very well with a value of $\Delta\theta_{\text{mosaic}} \approx 1.0 \times 10^{-6}$ implied by the 300 keV "inflexion point" for Si [660]. Using this estimate for $\Delta\theta_{\text{mosaic}}$ we would expect the "inflexion point" for Si [220] to occur at ≈ 1.5 MeV and for Si [880] to occur at ≈ 140 keV. Both of these are consistent with the data presently available. This quasimosaic width corresponds to 0.2″.

We conclude by noting that although the diffraction

Table 2
Theoretical values for the extinction lenght t_1 at 1 MeV for the specified reflections

Reflection	d(Å)	t_1(mm/MeV) [a]
Si[220]	1.92	0.6796
Si[440]	0.96	1.0733
Si[660]	0.64	1.967
Si[880]	0.48	3.718

[a] Form factors taken from Hartree–Fock calculations by DeMarco and Weiss [6].

linewidths were limited by finite source size to about 1″, the intrinsic resolution of the crystal was probably $\approx \times 5$ less. With the use of thinner sources (with contributions of 0.5″ instead of 1″), we may expect a significant improvement in instrument resolution. Such an improvement has important consequences in high resolution gamma-ray spectroscopy. Indeed, with a reflectivity that is constant up to 1.5 MeV in first order and only slightly decreasing from 680 keV on in second order, one might envisage to obtain routinely resolutions of 800 eV in first order and 400 eV in second order in the energy range of 1 MeV, values that were not thought about previously.

Acknowledgment

Some of the authors (E.K. and P.V.A.) owe a great debt of gratitude to L. Jacobs and M. Hart for selecting the set of high quality diffraction crystals. Part of this work was performed in the framework of the association between the University of Leuven and the SCK/CEN (Nuclear Energy Centre) in Mol with financial support from the Interuniversity Institute for Nuclear Science Belgium.

References

[1] L. Jacobs, Dissertation, Katholieke Universiteit Leuven (1977) unpublished.
[2] L. Jacobs and M. Hart, Nucl. Instr. and Meth. 114 (1977) 301.
[3] H.R. Koch et al., Nucl. Instr. and Meth. 175 (1980) 401.
[4] See for example W.H. Zachariasen, Theory of X-Ray Diffraction in Crystals (John Wiley, New York, 1945).
[5] O.I. Sumbayev, JETP Lett. 5 (1957) 1042.
[6] J.J. De Marco and R.J. Weiss, Phys. Rev. 137 (1965) 1869.